



Direction Aided Multipath Channel Estimation for Millimeter Wave Systems

Downloaded from: <https://research.chalmers.se>, 2026-04-04 03:48 UTC

Citation for the original published paper (version of record):

Koirala, R., Uguen, B., Dardari, D. et al (2021). Direction Aided Multipath Channel Estimation for Millimeter Wave Systems. IEEE Vehicular Technology Conference, 2021-April.
<http://dx.doi.org/10.1109/VTC2021-Spring51267.2021.9448770>

N.B. When citing this work, cite the original published paper.

© 2021 IEEE. Personal use of this material is permitted. Permission from IEEE must be obtained for all other uses, in any current or future media, including reprinting/republishing this material for advertising or promotional purposes, or reuse of any copyrighted component of this work in other works.

Direction Aided Multipath Channel Estimation for Millimeter Wave Systems

Remun Koirala^{*†‡}, Bernard Uguen[‡], Davide Dardari[†], Henk Wymeersch[§] and Benoît Denis^{*}

^{*}CEA-Leti Minatec Campus, 17 rue des Martyrs, 38054 Grenoble Cedex 09, France

[†]DEI-CNIT, University of Bologna, via dell'Università 52, I-47521 Cesena (FC), Italy

[‡]University of Rennes 1-IETR (CNRS UMR 6164), Av. du General Leclerc, 35042, Rennes, France

[§]Department of Electrical Engineering, Chalmers University of Technology, Gothenburg, Sweden

Abstract—In this paper, we present a low-latency direction assisted channel estimation algorithm suitable for millimeter wave (mm-Wave) systems. First, during the beam training procedure, we perform angle of departure (AoD) and angle of arrival (AoA) measurements with their corresponding variances and based on them, we design both downlink and uplink beams. We then perform signal measurements with these beams and accordingly design the sensing matrix, while also iteratively refining the angle estimation and the beams for the next measurements accordingly. Finally, exploiting both the sparseness and the intrinsic geometric nature of the mm-Wave channel, we apply compressive sensing tools so as to complete the estimation procedure. Simulations show that the corresponding estimation error decreases rapidly in comparison with other conventional approaches.

I. INTRODUCTION

The millimeter wave (mm-Wave) technology has been touted as a strong contender to accommodate the rapidly burgeoning demands for both data traffic and throughput in the new fifth generation (5G) of cellular systems [1]. The motive behind this choice is clear: operating in the millimeter wave (mm-Wave) band (typically, at a central frequency > 24 GHz) offers a huge amount of unlicensed bandwidth, and hence, the opportunity to multiplex high data rates among multiple users at the same time. Moving up the mm-Wave spectrum does not come without complications, however. The propagation characteristics of radio signals at such high frequencies proves to be a serious impediment to the advantages mentioned above. These signals are indeed affected by severe power pathloss, additional propagation losses due to specific environmental conditions (e.g., rain, fog) and even more importantly, radio blockages [2], [3].

On the other hand, transmitting signals of shorter wavelengths like in mm-Wave allows for smaller antenna sizes [4]. Exploiting this reduced size, instead of using only one antenna, a large number of antenna elements can thus be integrated on both sides of the radio link to concentrate the signal power in specific directions of space and overcome signal attenuation, what is also known as beamforming [5]. One major challenge of mm-Wave beamforming (and beyond, of beam alignment) is that the transmitter needs to have a fairly good knowledge of channel information with respect to the receiver so as to transmit the beam with the adequate width in the right

direction. In this demanding context, channel estimation is thus of the highest importance.

In the literature, this mm-Wave channel estimation problem has been addressed from the perspective of two distinct stages, namely the beam training stage and the estimation algorithm stage. Firstly, for the beam training stage, the most straightforward approach is to exhaustively search the best beams in terms of received power, by testing all possible angular directions on both transmitter's and receiver's sides [6]. In contrast, [7] and [8] propose iterative multi-resolution beam training procedures, where larger beams are used first, before converging iteratively to a beam width corresponding to the a priori required spatial resolution. Likewise [9] proposes a similar iterative beam training process in presence of prior location information fed by angle of departure (AoD) and angle of arrival (AoA), significantly reducing the estimation latency. In [10], the authors devise a channel estimation strategy employing distinct beam patterns in different directions. The latter two strategies reduce the channel estimation duration, which is critical in case of 5G applications due to their both low latency requirements and the necessity to operate at mm-Wave, possibly under mobility. Secondly, in the estimation stage, most of the contributions are based on compressive sensing techniques, exploiting the aforementioned sparsity of the channel, with algorithms such as orthogonal matching pursuit (OMP) [11]–[13], simultaneous orthogonal matching pursuit (SOMP) [14] and L1-norm minimization [15].

In this paper, we mainly consider the beam training stage and study how directional information, in particular, angular measurements can be used to further assist channel estimation. Our main motivation is to minimize the number of searches (and hence the duration) performed by the transmitter and the receiver beam pair in the conventional methods. Due to the sparse and geometric nature of the mm-Wave channel, the exploitation of such angular information is indeed expected to be beneficial to estimation, especially in terms of latency.

II. SYSTEM MODEL

A. Deployment scenario

Consider a mm-Wave downlink scenario with a base station (BS) and a user, equipped respectively with N_t antennas and

N_r antennas and operating at the carrier frequency f_c (and the corresponding wavelength λ_c) with bandwidth B , and K scatterers, as illustrated in Fig. 1. The BS, the user and the k -th scatterer are located at positions $\mathbf{q} = [q_x, q_y]^T$, $\mathbf{p} = [p_x, p_y]^T$ and $\mathbf{s}_k = [s_{k,x}, s_{k,y}]^T$ respectively. The position of the BS is assumed to be known, whereas that of both user and the scatterers are unknown a priori. The BS is assumed to have a known orientation, whereas the user is arbitrarily oriented towards an angle $o \in (0, 2\pi]$ with respect to the reference x -axis (as indicated in the figure).

B. Channel model

The $N_r \times N_t$ complex channel matrix between the BS and the user is denoted by \mathbf{H} and is formulated as in [8].

$$\mathbf{H} = \sqrt{\frac{N_r N_t}{\rho}} \sum_{k=0}^K h_k e^{-\frac{j2\pi\tau_k}{T_s}} \mathbf{a}_{\text{Rx}}(\phi_k) \mathbf{a}_{\text{Tx}}^H(\theta_k), \quad (1)$$

where ρ is the average path-loss term, h_k , $\tau_k = d_k/c$ (with c , the speed of light), θ_k and ϕ_k are respectively the complex channel coefficient, the time delay, the AoD and the AoA of the k -th path between the BS and the user, $T_s = 1/B$ is the sampling period, $\mathbf{a}_{\text{Tx}}(\theta_k) \in \mathbb{C}^{N_t}$ and $\mathbf{a}_{\text{Rx}}(\phi_k) \in \mathbb{C}^{N_r}$ are the antenna array response vectors at the BS and the user respectively. Similarly to [14], we can define

$$\theta_k = \begin{cases} \arccos\left(\frac{p_x - q_x}{\|\mathbf{p} - \mathbf{q}\|_2}\right) & k = 0 \\ \arccos\left(\frac{s_{k,x} - q_x}{\|\mathbf{s}_k - \mathbf{q}\|_2}\right) & \text{otherwise,} \end{cases} \quad (2a)$$

$$\phi_k = \begin{cases} \pi + \arccos\left(\frac{p_x - q_x}{\|\mathbf{p} - \mathbf{q}\|_2}\right) - o & k = 0 \\ \pi - \arccos\left(\frac{p_x - s_{k,x}}{\|\mathbf{p} - \mathbf{s}_k\|_2}\right) - o & \text{otherwise,} \end{cases} \quad (2b)$$

Considering a uniform linear array (ULA) model for the antenna array, we can express $\mathbf{a}_{\text{Tx}}(\theta_k)$ as

$$\mathbf{a}_{\text{Tx}}(\theta_k) = \frac{1}{\sqrt{N_t}} [1, e^{j\frac{2\pi}{\lambda_c} d \cos(\theta_k)}, \dots, e^{j(N_t-1)\frac{2\pi}{\lambda_c} d \cos(\theta_k)}]^T. \quad (3)$$

where d is the distance between two antenna elements. Similarly, we can formulate $\mathbf{a}_{\text{Rx}}(\phi_k)$ by replacing N_t with N_r and θ_k with ϕ_k in equation (3).

We can reformulate equation (1) similarly to [8] as

$$\mathbf{H} = \sqrt{\frac{N_r N_t}{\rho}} \mathbf{A}_{\text{Rx}} \mathbf{\Lambda} \mathbf{A}_{\text{Tx}}^H, \quad (4)$$

where,

$$\mathbf{A}_{\text{Tx}} = [\mathbf{a}_{\text{Tx}}(\theta_0), \dots, \mathbf{a}_{\text{Tx}}(\theta_K)], \quad (5a)$$

$$\mathbf{A}_{\text{Rx}} = [\mathbf{a}_{\text{Rx}}(\phi_0), \dots, \mathbf{a}_{\text{Rx}}(\phi_K)], \quad (5b)$$

$$\mathbf{\Lambda} = \text{diag}\left(h_0 e^{-\frac{j2\pi\tau_0}{T_s}}, \dots, h_K e^{-\frac{j2\pi\tau_K}{T_s}}\right). \quad (5c)$$

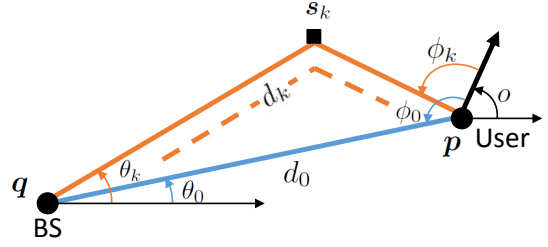


Fig. 1: Illustration of the system model with a BS, a user and k -th scatterer located at positions \mathbf{q} , \mathbf{p} and \mathbf{s}_k respectively. The orientation of the user is indicated by an angle o with respect to the reference x -axis. The distance between the BS and the user through direct path is d_0 and through the k -th scatterer is d_k . The AoD and AoA for the k -th path are θ_k and ϕ_k respectively.

C. Communication model

Consider a downlink scenario between the BS and the user. If the BS uses a beamforming vector \mathbf{f}_p and the mobile device uses a combining vector \mathbf{w}_q , the resulting received signal can be written as:

$$y_{q,p} = \mathbf{w}_q^H \mathbf{H} \mathbf{f}_p s_p + n_{q,p}, \quad (6)$$

where, s_p is the transmitted symbol such that $\mathbb{E}[s_p] = P_{\text{Tx}}$, where P_{Tx} is the average power used per transmission, and $n_{q,p}$ is a Gaussian distributed noise with zero mean and bilateral power spectrum density $N_0/2$ per real dimension. Considering M_B and M_U of such beamforming and combining vectors respectively, the received signal can be written as

$$\mathbf{Y} = \mathbf{W}^H \mathbf{H} \mathbf{F} \mathbf{S} + \mathbf{N}, \quad (7)$$

where $\mathbf{W} = [\mathbf{w}_1, \mathbf{w}_2, \dots, \mathbf{w}_{M_U}]$ and $\mathbf{F} = [\mathbf{f}_1, \mathbf{f}_2, \dots, \mathbf{f}_{M_B}]$. Similarly to [8], for the channel estimation phase, we assume all the transmitted symbols are equal *i.e.* $\mathbf{S} = \sqrt{P_{\text{Tx}}} \mathbf{I}_{M_B}$, where \mathbf{I} is an identity matrix of size M_B , and hence

$$\mathbf{Y} = \sqrt{P_{\text{Tx}}} \mathbf{W}^H \mathbf{H} \mathbf{F} + \mathbf{N}. \quad (8)$$

D. AoD and AoA estimation

We assume that the BS and the user have access to an estimator of the AoD (θ_k) and AoA (ϕ_k) respectively for every path¹. Hence, for the k -th path, the estimated AoD and AoA can be expressed as:

$$\hat{\theta}_k = \theta_k + e_{\theta_k}, \quad (9a)$$

$$\hat{\phi}_k = \phi_k + e_{\phi_k}, \quad (9b)$$

where, e_{θ_k} and e_{ϕ_k} are the estimation errors regarding θ_k and ϕ_k respectively. It was shown in [18] that under conditions such as a large number of transmit and receive antennas and a

¹The angle estimations can be realized through well known subspace based AoA estimators [16] such as Multiple Signal Classification (MUSIC) or Estimation of Signal Parameters via Rotational Invariance Technique (ESPRIT). The BS can estimate the AoA with downlink measurements. Considering that for a given path, the AoD from the perspective of BS in downlink is the same as the AoA from the perspective of the user in uplink, the user can estimate θ_k with uplink AoA measurements. Hence, in this paper, the term estimated AoD refers to the estimated uplink AoA. The sparse nature of the mm-Wave channel means that there are few distinct paths and the angle in each path can be estimated with high resolution due to the large number of antenna elements [17]

large bandwidth, which is reasonable in mm-Wave, the error for both AoD and AoA can be assumed as independent per path. Moreover, we assume that the random measurement noise terms are Gaussian distributed with zero mean and known variances² σ_θ^2 and σ_ϕ^2 [19].

III. DIRECTION AIDED CHANNEL ESTIMATION

The objective of channel estimation is to estimate the matrix \mathbf{H} in a multipath scenario. Equivalently, one can estimate the channel coefficient and the three location dependent variables (i.e., delay, AoD and AoA) for each path. In this section, we firstly express the channel estimation problem as a sparse problem. We then introduce the sectorized beamforming model to simplify the previous channel estimation problem. Finally, we propose the direction aided channel estimation algorithm.

A. Channel estimation problem

Vectorizing equation (8), we can write

$$\mathbf{y}_v = \text{vec}(\mathbf{Y}) = \sqrt{P_t} \text{vec}(\mathbf{W}^H \mathbf{H} \mathbf{F}) + \text{vec}(\mathbf{N}), \quad (10a)$$

$$= \zeta(\mathbf{F}^T \otimes \mathbf{W}^H)(\mathbf{A}_{\text{Tx}}^* \otimes \mathbf{A}_{\text{Rx}}) \text{vec}(\mathbf{\Lambda}) + \mathbf{n}_v, \quad (10b)$$

$$= \zeta(\mathbf{F}^T \mathbf{A}_{\text{Tx}}^* \otimes \mathbf{W}^H \mathbf{A}_{\text{Rx}}) \mathbf{x} + \mathbf{n}_v. \quad (10c)$$

where $\zeta = \sqrt{N_r N_t P_t} / \rho$, $\mathbf{x} = \text{vec}(\mathbf{\Lambda})$ and $\mathbf{n}_v = \text{vec}(\mathbf{N})$.

In order to present a sparse formulation of the estimation problem, consider a grid of N_B discrete AoD and N_U AoA directions taken uniformly between 0 and 2π , with the i -th grid direction represented by $\tilde{\theta}_i$ and $\tilde{\phi}_i$ for AoD and AoA respectively. Mathematically, $\tilde{\theta}_i = 2\pi(i-1)/N_B$ and $\tilde{\phi}_i = 2\pi(i-1)/N_U$. Assume,

$$\tilde{\mathbf{A}}_{\text{Tx}} = [\mathbf{a}_{\text{Tx}}(\tilde{\theta}_1), \dots, \mathbf{a}_{\text{Tx}}(\tilde{\theta}_{N_B})], \quad (11a)$$

$$\tilde{\mathbf{A}}_{\text{Rx}} = [\mathbf{a}_{\text{Rx}}(\tilde{\phi}_1), \dots, \mathbf{a}_{\text{Rx}}(\tilde{\phi}_{N_U})]. \quad (11b)$$

Similarly to [8, equation (17)], we can now reformulate equation (10c) as a sparse problem:

$$\mathbf{y}_v = \zeta(\mathbf{F}^T \tilde{\mathbf{A}}_{\text{Tx}}^* \otimes \mathbf{W}^H \tilde{\mathbf{A}}_{\text{Rx}}) \mathbf{x} + \mathbf{n}_v = \zeta \mathbf{M} \mathbf{x} + \mathbf{n}_v, \quad (12)$$

where \mathbf{M} is the sensing matrix and the k -th element in \mathbf{y}_v is

$$y_k = \zeta(\mathbf{f}_p^T \tilde{\mathbf{A}}_{\text{Tx}}^* \otimes \mathbf{w}_q^H \tilde{\mathbf{A}}_{\text{Rx}}) \mathbf{x} + n_k = \zeta \mathbf{M}(k, :) \mathbf{x} + n_k, \quad (13)$$

where the k -th measurement is performed with the beamforming vector \mathbf{f}_p and the combining vector \mathbf{w}_q , and $\mathbf{M}(k, :)$ represents the k -th row of the sensing matrix. Likewise

$$\mathbf{f}_p^T \tilde{\mathbf{A}}_{\text{Tx}}^* = [\mathbf{a}_{\text{Tx}}^H(\tilde{\theta}_1) \mathbf{f}_p, \dots, \mathbf{a}_{\text{Tx}}^H(\tilde{\theta}_{N_B}) \mathbf{f}_p], \quad (14a)$$

$$\mathbf{w}_q^H \tilde{\mathbf{A}}_{\text{Rx}} = [\mathbf{w}_q^H \mathbf{a}_{\text{Rx}}(\tilde{\phi}_1), \dots, \mathbf{w}_q^H \mathbf{a}_{\text{Rx}}(\tilde{\phi}_{N_U})]. \quad (14b)$$

Equation (14a) (and equivalently, equation (14b)) represents the gain due to the beamforming vector \mathbf{f}_p in all the grid directions. Hence, $\mathbf{f}_p^T \tilde{\mathbf{A}}_{\text{Tx}}^* \otimes \mathbf{w}_q^H \tilde{\mathbf{A}}_{\text{Rx}}$ represents the gain due to \mathbf{f}_p and \mathbf{w}_q in all the BS and user grid combinations ($N_B \times N_U$ combinations).

²The variance of estimation depends on the estimator and factors such as signal-to-noise ratio (SNR), bandwidth and number of antenna elements. Such variances can be known a priori, by means of e.g., theoretical bounds calculation, empirical statistics drawn over sequences of real measurements, or even through simulations.

B. Sectorized beamforming model

We approximate the actual beamforming by a *sectorized model* [20], where the transmitted and received beams are divided into two sectors, a main lobe³ sector whose antenna gain depends on the beamwidth ω and a side lobe sector with a fixed gain. The beamwidth is inversely proportional to the number of antenna elements.

Accordingly, in the sectorized model, the antenna gain $G_x(\omega_x)$, where $x \in \{\text{Tx}, \text{Rx}\}$ at the BS side i.e. $\mathbf{f}^H \mathbf{a}_{\text{Tx}}(\theta_k)$ and user side i.e. $\mathbf{w}^H \mathbf{a}_{\text{Rx}}(\phi_k)$ can be approximated similarly to [8], [21]

$$G_x(\omega_x) = \begin{cases} \gamma_x(\omega_x) = G_0 \frac{2\pi - (2\pi - \omega_x)\epsilon}{\omega_x}, & \text{in the main lobe,} \\ g = G_0 \epsilon, & \text{otherwise,} \end{cases} \quad (15)$$

where G_0 is the antenna gain of an equivalent omni-directional beam (i.e., $\omega_x = 2\pi$) and ϵ is a small positive constant $\ll 1$.

C. Sensing matrix design

From equations (13) and (15), each element of the sensing matrix \mathbf{M} in (12) can have four distinct values: $\gamma_{\text{Tx}}(\omega_{\text{Tx}}) \gamma_{\text{Rx}}(\omega_{\text{Rx}})$, $\gamma_{\text{Tx}}(\omega_{\text{Tx}}) g$, $g \gamma_{\text{Rx}}(\omega_{\text{Rx}})$ and g^2 depending on the beam alignment and beamwidths.

Consider an example scenario as illustrated in Fig. 2 with a BS, a user and two paths: a direct path and an indirect path through \mathbf{s}_1 . The complex channel coefficient of direct path h_0 is indicated by α_0 and that of indirect path h_1 is α_1 . Consider equi-spaced grids at both BS and user with $N_B = N_U = 8$ with $\tilde{\theta}_i = \tilde{\phi}_i = 2\pi(i-1)/8$ for all natural numbers $i \leq 8$.

We have beams from the BS and the user with widths ω_{Tx} and ω_{Rx} respectively, both directed at a scatterer located at \mathbf{s}_1 . Let $\mathbf{m}_{\text{BS}} = \mathbf{f}^T \tilde{\mathbf{A}}_{\text{Tx}}^*$ and $\mathbf{m}_{\text{MS}} = \mathbf{w}^H \tilde{\mathbf{A}}_{\text{Rx}}$. As illustrated in the figure, only the indirect path is covered by the main lobes of both BS and user side beams. Then, the received signal composed of two paths can be expressed as follows:

$$y = \zeta \sum_{k=0}^1 G_{\text{Rx}}(\omega_{\text{Rx},k}) G_{\text{Tx}}(\omega_{\text{Tx},k}) \alpha_k + n, \quad (16a)$$

$$= \zeta [\gamma_{\text{Tx}}(\omega_{\text{Tx},1}) \gamma_{\text{Rx}}(\omega_{\text{Rx},1}) \alpha_1 + g^2 \alpha_0] + n, \quad (16b)$$

and each row of the sensing matrix for the given beam pair can be calculated as

$$\mathbf{m}_{\text{Tx}} = [g, \gamma_{\text{Tx}}(\omega_{\text{Tx}}), g, g, g, g, g, g], \quad (17a)$$

$$\mathbf{m}_{\text{Rx}} = [g, g, g, \gamma_{\text{Rx}}(\omega_{\text{Rx}}), g, g, g, g], \quad (17b)$$

$$\mathbf{M}(k, :) = \mathbf{m}_{\text{Tx}} \otimes \mathbf{m}_{\text{Rx}}. \quad (17c)$$

D. Beam design

The key to efficiently solving the sparse problem in (12) is to obtain the right measurements. In order to do so, based on the angle estimates from equation (9), for each path, we design the optimal beamwidth ω_{Tx} and ω_{Rx} at both BS and user respectively in such a way as to minimize the beam

³Here, the term main lobe stands for the angular region of the antenna pattern centered around the axis of maximum gain and aperture equal to the half-power beamwidth of the pattern.

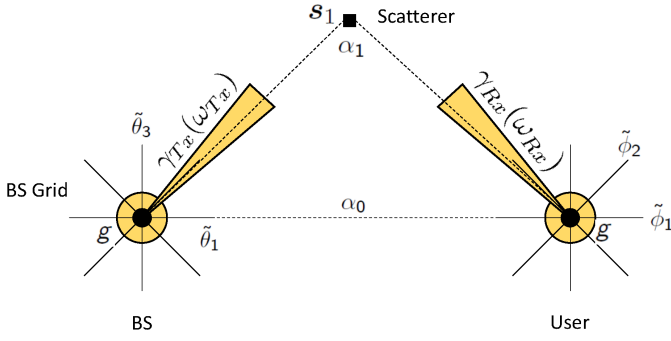


Fig. 2: Example scenario with $N_B = N_U = 8$ with both BS and user main lobe directed towards s_1 .

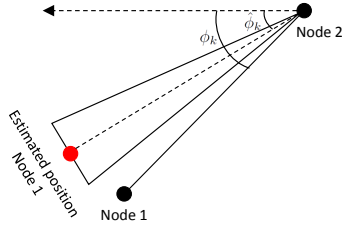


Fig. 3: Illustration of beam misalignment error due to erroneous estimation of $\hat{\phi}_k$ such that Node 1 is not within the transmitted beam. Node 1 might be receiver or scatterer depending on whether it corresponds to the direct path or not.

misalignment error per path. We define the misalignment error as the event that the scatterer (or correspondingly the receiving node in case of direct path transmission) doesn't fall within the main beam lobes of either transmitting or receiving nodes due to estimation errors. This event is depicted in Fig. 3.

Based on this definition of the misalignment error, we design the beamwidth⁴ $\omega_{\text{Tx},k}$ with respect to the k -th path such that the probability of misalignment error is a constant ϵ_{Tx} , i.e.,

$$\mathcal{P}\left(\hat{\theta}_k - \frac{\omega_{\text{Tx},k}}{2} \leq \theta \leq \hat{\theta}_k + \frac{\omega_{\text{Tx},k}}{2}\right) = \epsilon_{\text{Tx}}. \quad (18)$$

Accordingly,

$$\omega_{\text{Tx},k} = 2\Phi^{-1}\left(\frac{\epsilon_{\text{Tx}} + 1}{2}\right)\sigma_{\theta}, \quad (19)$$

where, $\Phi^{-1}(x)$ is the inverse function of the cumulative distribution function (CDF) of standard normal distribution. Likewise,

$$\omega_{\text{Rx},k} = 2\Phi^{-1}\left(\frac{\epsilon_{\text{Rx}} + 1}{2}\right)\sigma_{\phi}. \quad (20)$$

In the above equations, we use the relations from equations (9a) and (9b), where $\hat{\theta}_k$ and $\hat{\phi}_k$ are normally distributed around the true AoD and AoA for each k -th path.

⁴In practice, the ability of an antenna to beamform with a certain width depends on the number and the geometry of the antenna elements. In our scenario, we assume that both BS and user have enough elements to support a small beamwidth. In the context of ULA, the minimum number of antenna elements required to achieve a beamwidth ω can be approximated [22, Equation 1.9] as $1.8/\omega$. Then to achieve other larger beamwidths, we can select the required number of antenna elements according to the optimization problem formulated in [23], [24].

E. Direction aided channel estimation algorithm

The overall direction aided channel estimation algorithm can be summarized by the following steps.

Output: \hat{H}

Initialization:

- 1: Initial estimates of AoD $\hat{\theta}_k^{(1)}$ and AoA $\hat{\phi}_k^{(1)}$ at the BS and user respectively for all the $(K + 1)$ paths and their corresponding variances $\sigma_{\hat{\theta}_k}^2$ and $\sigma_{\hat{\phi}_k}^2$.
- 2: $i = 1$

Beam Training Phase:

- 3: **while** terminating condition⁵ is not satisfied **do**
- 4: **for all** $\hat{\theta}_{k_1}^{(i)}$ and $\hat{\phi}_{k_2}^{(i)}$ pair $\forall k_1, k_2 \in \{0, 1, \dots, K\}$ **do**
- 5: Calculate the beamwidth $\omega_{\text{Tx},k_1}^{(i)}$ and $\omega_{\text{Rx},k_2}^{(i)}$ for BS and user beams according to equations (19) and (20) respectively.
- 6: Set the BS and user beams towards $\hat{\theta}_{k_1}^{(i)}$ and $\hat{\phi}_{k_2}^{(i)}$ respectively with widths $\omega_{\text{Tx},k_1}^{(i)}$ and $\omega_{\text{Rx},k_2}^{(i)}$.
- 7: With these beams, generate the received signal y_i , according to equation (16a).
- 8: Calculate the corresponding row of the sensing matrix $M(i, :)$, as in equation (17c).
- 9: **if** $|y_i|^2 \geq \gamma_i$ **then**
- 10: With downlink transmission towards $\hat{\theta}_{k_1}^{(i)}$ with beamwidth $\omega_{\text{Tx},k_1}^{(i)}$, the BS estimates the refined AoA $\hat{\phi}_k^{(i+1)}$.
- 11: With uplink transmission towards $\hat{\phi}_{k_1}^{(i)}$ with beamwidth $\omega_{\text{Tx},k_1}^{(i)}$, the user estimates the refined AoD $\hat{\theta}_k^{(i+1)}$.
- 12: Update the estimation variances $\sigma_{\hat{\theta}_k}^2$ and $\sigma_{\hat{\phi}_k}^2$.
- 13: **end if**
- 14: $i = i + 1$
- 15: **end for**
- 16: **end while**

Estimation Algorithm Phase:

- 17: $z = \text{OMP}(M, y)$ and reshape z from $N_B N_U \times 1$ vector to a $N_B \times N_U$ matrix.

$$\hat{\Lambda} = \text{reshape}(z, [N_B, N_U]). \quad (21)$$

$$18: \hat{H} = \tilde{A}_{\text{Rx}} \hat{\Lambda} \tilde{A}_{\text{Tx}}^H$$

19: **return** \hat{H}

In summary, we firstly initialize the algorithm with coarse estimates of the AoDs and AoAs along with their variances for all the paths. For each AoD and AoA, we then calculate the beamwidth such that we limit the misalignment error probabilities to ϵ_{Tx} and ϵ_{Rx} at the transmitter and the receiver respectively. We then sequentially transmit for every pair of AoD and AoA, in total $(K + 1)^2$ pairs, with the newly calculated beamwidth and measure the received signal and the corresponding row of the sensing matrix according to equations (16a) and (17c) respectively. Following, we refine

⁵The terminating condition can be application dependent. It can be, for e.g., the minimum beamwidth constraint, the total channel estimation duration constraint, etc.

AoDs and AoAs, as well as their corresponding variances, for each path with the new beamwidth. We only perform this step if the BS and user beam pairs are corresponding to either the direct path or the same scatterer, hence $K + 1$ times. In order to decide when to perform this step, we threshold the received signal power on γ_i , which is a function of $\omega_{\text{Tx},k_1}^{(i)}$ and $\omega_{\text{Rx},k_2}^{(i)}$, such that we only measure the angles when both the main lobes are aligned towards either each other or the same scatterer. This beam refining and measuring process is iteratively repeated until some application dependent terminating condition is fulfilled. The sparsity of mm-Wave channel ensures that the sensing matrix is sparse, and hence we use some compressive sensing algorithm such as OMP [13] in this case to finally estimate the channel.

IV. NUMERICAL RESULTS

In our work, we assume an analog beamforming architecture on both BS and user sides with only 1 radio-frequency (RF) chain operating at $f_c = 28$ GHz with bandwidth $B = 500$ MHz. We assume the transmit power $P_t = 30$ dBm and the noise power density at the received signal $N_0 = -174$ dBm. We consider 1 BS with known position ($\mathbf{q} = [0, 0]^T$) and orientation ($\phi = 0^\circ$), and $K = 3$ scatterers (and accordingly, 4 paths). Moreover, we assume the $N_B = N_U = 360$ grid points at both the BS and the user respectively. For determining the beamwidth, we consider $\epsilon_{\text{Tx}} = \epsilon_{\text{Rx}} = 0.99$.

We compare our proposed direction assisted channel estimation method with that resulting from two well-known solutions, namely exhaustive search and iterative multi-resolution search [6], [8]. For the exhaustive search, we consider the beamwidth of the BS and the user to be fixed and equal to $\omega_{\text{Tx}}^{\text{Ex}}$ and $\omega_{\text{Rx}}^{\text{Ex}}$. Thus, the BS and the user go through all the possible combinations of beams throughout the search area with the width in order to complete the beam training process. On the other hand, for the case of iterative multi-resolution based search, we implement the multipath channel estimation algorithm in [8], where we start with an initial beamwidth of $\pi/2$ rad and iteratively bisect the beamwidth and sweep to converge to finer resolution. We assume that each transmission can be completed within $14.3\mu\text{s}$ which is equal to one orthogonal frequency division multiplexing (OFDM) symbol length [25]. For the case of the proposed direction aided method, we choose the minimum beamwidth constraint at both BS and user's end as terminating condition for the algorithm *i.e.* the algorithm terminates when the refined beamwidth reaches 1 degree at both the ends for all different AoDs and AoAs. This minimum beamwidth requirement corresponds to the minimum number of antenna requirement of 104. With this consideration, we assume $N_t = N_r = 128$. We characterize the error in channel estimation in terms of normalized mean square error (NMSE), defined as $\text{NMSE} = \|\mathbf{H} - \hat{\mathbf{H}}\|_2^2 / \|\mathbf{H}\|_2^2$, where, $\|\cdot\|_2$ represents the 2-norm.

In Fig. 4, we can see the minimum beamwidth that can be achieved within a given duration. For instance, during $x \mu\text{s}$, we can transmit $n = \lfloor x/14.3 \rfloor$ beam pairs. For the case of exhaustive search based channel estimation, since we

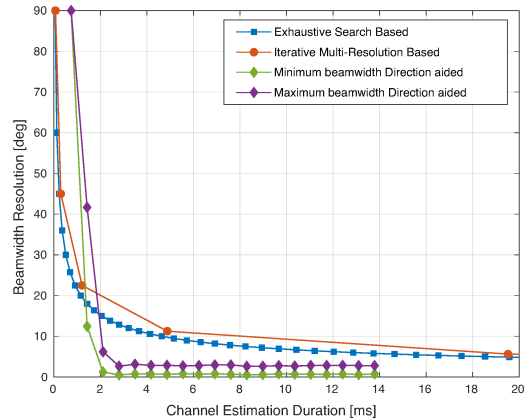


Fig. 4: Beamwidth achieved for different channel estimation methods varied with total channel estimation duration

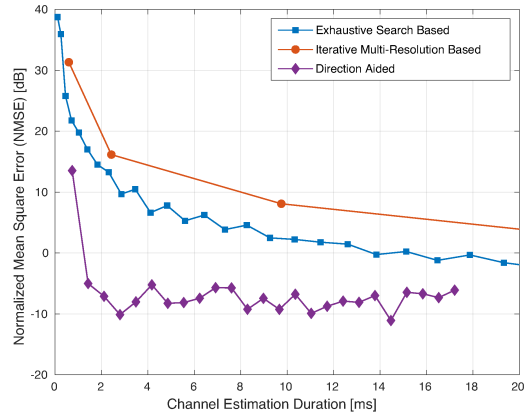


Fig. 5: NMSE comparison for different channel estimation methods varied with total channel estimation duration

need to search the entire $\pi/2$ space in $x \mu\text{s}$, the minimum beamwidth that we can use is $\omega_{\text{Tx}}^{\text{Ex}} = \omega_{\text{Rx}}^{\text{Ex}} = \pi/2n$ rad. In case of iterative search, the minimum beamwidth we can achieve during n steps is given by $\omega_{\text{Tx}}^{\text{It}} = \omega_{\text{Rx}}^{\text{It}} = \pi/2 \log_2(n)$, since the search sector grows to the power of 2 at each bisection. For the direction based method, the minimum beamwidth with n possible beam pairs depends on how fast the beamwidth converges at each iteration and hence, on the variance of estimated AoD and AoA. Since the previous variances, and thus the beamwidths, vary for each path, for the proposed direction aided method, we plot both the minimum and maximum beamwidths allocated at each iteration. In our simulations, in order to have a closed form expression, we assume Cramer Rao Lower Bound (CRLB) as the angle estimation variance⁶ when estimating the AoD and AoA, as derived in [14]. In Fig. 4 we can see that the beamwidth in the proposed direction assisted algorithm decreases much more quickly than in other cases.

In Fig. 5, we also present the NMSE of channel estimation for each method for different channel estimation duration and

⁶Although CRLB represents a lower bound on the variance of an unbiased estimator and hence, the best case scenario, the authors in [14] show that it is possible for an estimator to achieve the bound even at low SNR.

with different beamwidths corresponding to the estimation duration, as shown in Fig. 4. In this figure, we can observe that with the proposed direction aided method, the estimation error, similar to the beamwidth, decreases more rapidly than the other methods. The reason for this is that in the proposed method, we use directly the relevant beams even though there is a small probability of misalignment. However, in the exhaustive and iterative search based methods, a lot of time is spoilt while searching all the sectors including those which do not provide any relevant information. This gain in latency could be crucial especially in the context of low latency 5G applications and in dynamic channel estimation scenarios, for e.g., tracking a mobile user.

V. CONCLUSIONS

In this paper, we have presented a low latency solution for channel estimation in the context of mm-Wave systems, with the aid of direction information. Exploiting the inherently sparse properties of the mm-Wave channel, where the number of multipath components is limited, as well as AoD and AoA estimation for each path, we show that the direction aided method outperforms other existing methods such as the exhaustive and iterative multi-resolution search based channel estimation approaches. Simulation results in a canonical scenario illustrate some latency gains accordingly. In future works, we will consider coupling the proposed mm-Wave multipath channel estimation method with angle-based simultaneous localization and mapping algorithms.

ACKNOWLEDGMENT

This work was supported, in part, by the European H2020 project SECREDAS, which is funded through the specific ECSEL Joint Undertaking research and innovation program (GA No. 783119), and by the Swedish Research Council under grant No. 2018-03701.

REFERENCES

- [1] T. S. Rappaport, S. Sun, R. Mayzus, H. Zhao, Y. Azar, K. Wang, G. N. Wong, J. K. Schulz, M. Samimi, and F. Gutierrez, "Millimeter wave mobile communications for 5G cellular: It will work!" *IEEE Access*, vol. 1, pp. 335–349, 2013.
- [2] F. Al-Ogaili and R. M. Shubair, "Millimeter-wave mobile communications for 5G: Challenges and opportunities," in *2016 IEEE International Symposium on Antennas and Propagation (APSURSI)*, Jun 2016, pp. 1003–1004.
- [3] Y. Niu, Y. Li, D. Jin, L. Su, and A. V. Vasilakos, "A survey of millimeter wave communications (mmwave) for 5g: opportunities and challenges," *Wireless Networks*, vol. 21, no. 8, pp. 2657–2676, Nov. 2015. [Online]. Available: <https://doi.org/10.1007/s11276-015-0942-z>
- [4] P.-S. Kildal, *Foundations of antenna engineering: a unified approach for line-of-sight and multipath*. Artech House, 2015.
- [5] S. Sun, T. S. Rappaport, R. W. Heath, A. Nix, and S. Rangan, "MIMO for millimeter-wave wireless communications: beamforming, spatial multiplexing, or both?" *IEEE Communications Magazine*, vol. 52, no. 12, pp. 110–121, Dec 2014.
- [6] "IEEE standard for information technology–telecommunications and information exchange between systems–local and metropolitan area networks–specific requirements–part 11: Wireless lan medium access control (MAC) and physical layer (PHY) specifications amendment 3: Enhancements for very high throughput in the 60 GHz band," *IEEE Std 802.11ad-2012 (Amendment to IEEE Std 802.11-2012, as amended by IEEE Std 802.11ae-2012 and IEEE Std 802.11aa-2012)*, pp. 1–628, Dec 2012.
- [7] S. Hur, T. Kim, D. J. Love, J. V. Krogmeier, T. A. Thomas, and A. Ghosh, "Millimeter wave beamforming for wireless backhaul and access in small cell networks," *IEEE Transactions on Communications*, vol. 61, no. 10, pp. 4391–4403, Oct 2013.
- [8] A. Alkhateeb, O. E. Ayach, G. Leus, and R. W. Heath, "Channel estimation and hybrid precoding for millimeter wave cellular systems," *IEEE Journal of Selected Topics in Signal Processing*, vol. 8, no. 5, pp. 831–846, Oct. 2014.
- [9] N. Garcia, H. Wymeersch, E. G. Strm, and D. Slock, "Location-aided mm-wave channel estimation for vehicular communication," in *2016 IEEE 17th International Workshop on Signal Processing Advances in Wireless Communications (SPAWC)*, July 2016, pp. 1–5.
- [10] M. Kokshoorn, H. Chen, P. Wang, Y. Li, and B. Vucetic, "Millimeter wave MIMO channel estimation using overlapped beam patterns and rate adaptation," *IEEE Transactions on Signal Processing*, vol. 65, no. 3, pp. 601–616, Feb 2017.
- [11] A. Alkhateeb, G. Leus, and R. W. Heath, "Compressed sensing based multi-user millimeter wave systems: How many measurements are needed?" in *2015 IEEE International Conference on Acoustics, Speech and Signal Processing (ICASSP)*, Apr 2015, pp. 2909–2913.
- [12] J. Lee, G. Gil, and Y. H. Lee, "Exploiting spatial sparsity for estimating channels of hybrid MIMO systems in millimeter wave communications," in *2014 IEEE Global Communications Conference*, Dec 2014, pp. 3326–3331.
- [13] T. T. Cai and L. Wang, "Orthogonal matching pursuit for sparse signal recovery with noise," *IEEE Transactions on Information Theory*, vol. 57, no. 7, pp. 4680–4688, 2011.
- [14] A. Shahmansoori, G. E. Garcia, G. Destino, G. Seco-Granados, and H. Wymeersch, "Position and orientation estimation through millimeter-wave MIMO in 5G systems," *IEEE Transactions on Wireless Communications*, vol. 17, no. 3, pp. 1822–1835, Mar 2018.
- [15] S. Malla and G. Abreu, "Channel estimation in millimeter wave MIMO systems: Sparsity enhancement via reweighting," in *2016 International Symposium on Wireless Communication Systems (ISWCS)*, Sep. 2016, pp. 230–234.
- [16] R. Schmidt, "Multiple emitter location and signal parameter estimation," *IEEE Transactions on Antennas and Propagation*, vol. 34, no. 3, pp. 276–280, March 1986.
- [17] H. Wymeersch, G. Seco-Granados, G. Destino, D. Dardari, and F. Tufvesson, "5G mmwave positioning for vehicular networks," *IEEE Wireless Communications*, vol. 24, no. 6, pp. 80–86, Dec 2017.
- [18] Z. Abu-Shaban, X. Zhou, T. Abhayapala, G. Seco-Granados, and H. Wymeersch, "Error bounds for uplink and downlink 3D localization in 5G millimeter wave systems," *IEEE Transactions on Wireless Communications*, vol. 17, no. 8, pp. 4939–4954, 2018.
- [19] J. Talvitie, M. Valkama, G. Destino, and H. Wymeersch, "Novel algorithms for high-accuracy joint position and orientation estimation in 5G mmwave systems," in *2017 IEEE Globecom Workshops (GC Wkshps)*, Dec 2017, pp. 1–7.
- [20] A. M. Hunter, J. G. Andrews, and S. Weber, "Transmission Capacity of ad hoc Networks with Spatial Diversity," *IEEE Trans. Wireless Commun.*, vol. 7, no. 12, pp. 5058–5071, Dec. 2008.
- [21] H. Shokri-Ghadikolaei, C. Fischione, G. Fodor, P. Popovski, and M. Zorzi, "Millimeter Wave Cellular Networks: A MAC Layer Perspective," *IEEE Trans. Wireless Commun.*, vol. 63, no. 10, pp. 3437–3458, Oct. 2015.
- [22] M. A. Richards, *Fundamentals of radar signal processing*. Tata McGraw-Hill Education, 2005.
- [23] G. E. Garcia, N. Garcia, G. Seco-Granados, E. Karipidis, and H. Wymeersch, "Fast in-band position-aided beam selection in millimeter-wave mimo," *IEEE Access*, vol. 7, pp. 142 325–142 338, 2019.
- [24] G. E. Garcia, G. Seco-Granados, E. Karipidis, and H. Wymeersch, "Transmitter beam selection in millimeter-wave MIMO with in-band position-aiding," *IEEE Transactions on Wireless Communications*, vol. 17, no. 9, pp. 6082–6092, 2018.
- [25] Y. Li, J. G. Andrews, F. Baccelli, T. D. Novlan, and J. C. Zhang, "Design and Analysis of Initial Access in Millimeter Wave Cellular Networks," *IEEE Trans. Wireless Commun.*, vol. 16, no. 10, pp. 6409–6425, Oct 2017.